Hindawi
Journal of Electrical and Computer Engineering
Volume 2023, Article ID 8864216, 14 pages
https://doi.org/10.1155/2023/8864216

Research Article

Intelligent Integrated Approach for Voltage Balancing Using Particle Swarm Optimization and Predictive Models

Jasim Ghaeb,[1] Ibrahim Al-Naimi ,[2] and Malek Alkayyali[3]

[1]*Mechatronics Engineering Department, Philadelphia University, Amman, Jordan*
[2]*Electrical and Computer Engineering Department, Sultan Qaboos University, Muscat, Oman*
[3]*Department of Mechanical Engineering, Clemson University, Clemson, USA*

Correspondence should be addressed to Ibrahim Al-Naimi; i.alnaimi@squ.edu.om

Received 2 January 2023; Revised 27 April 2023; Accepted 31 July 2023; Published 15 September 2023

Academic Editor: Rossano Musca

In this paper, an intelligent integrated approach is proposed to control the reactive power and restore the voltage balance in a three-phase power system using particle swarm optimization (PSO), Gaussian process regression (GPR), and support vector machine (SVM). The PSO algorithm is used in offline mode to determine the optimal set of firing angles for the thyristor-controlled-reactor (TCR) compensator according to the smallest fitness value required for voltage balancing. The optimum firing angles are then used to train the GPR and SVM regression models. The GPR and SVM models are finally used as a real-time controller to retrieve the voltage balance in online mode. A simulation model and experimental setup of the electrical power system are built. The modeled system consists of a 500 km long transmission line. The line is divided into three-pi sections to guarantee a real system response. Several simulation and practical case studies have been conducted to test and validate the capability of the proposed integrated approach in solving the voltage unbalance problem. The results have revealed the supreme ability of the proposed integrated approach to restore the voltage balance quickly (within 20 ms) and for a wide range of voltage unbalance factors (VUFs) (3.90–8.42%).

1. Introduction

Electrical power systems normally operate under balance conditions and regular three-phase voltages. In some circumstances, unbalance conditions influence the electrical power system and cause unbalance voltages. These conditions emerge when the three-phase loads are irregular or because of the asymmetries in the network topology. The unbalance voltages will inevitably degrade the performance, i.e., quality, of electrical power systems [1–3]. Additionally, the unbalance voltage conditions cause several system deficiencies such as electrical machine overheating, transformer overloading, high losses, and low stability of the power system [4–6]. The unbalance three-phase system can be decomposed into positive and negative sequence components. Several definitions for voltage unbalance are introduced. According to IEEE Std.1159–1195, the voltage unbalance is defined as the ratio between negative and positive sequence voltages [7].

Voltage balancing is critical in three-phase power systems to ensure efficient and reliable operation. Different voltage balancing techniques have been proposed to ensure that the voltages in the three phases of the system are equal, leading to better performance, improved energy efficiency, and reduced equipment damage [8]. The use of compensators such as static synchronous compensators (STATCOMs) has shown promising results in voltage balancing in three-phase power systems [9–11]. In the next section, an overview of recent developments and state-of-the-art techniques for voltage balancing in three-phase power systems will be presented.

2. Literature Review

Many research works have been proposed to detect and mitigate the voltage unbalance problem. The research work in [12] introduced the concept of E-STATCOMs, which are

static compensator devices that include energy storage systems. The authors proposed using a supercapacitor energy storage system (SCESS) in conjunction with a STATCOM for controlling transients in a power system to improve reactive power unbalance following a contingency. The authors demonstrated that supplementary PI controllers in voltage magnitude and phase angle loops can provide extra damping to the system, leading to very good responses even under severe three-phase fault conditions. In [13], a method for controlling a 3-phase cascaded H-bridge (3ph-CHB) converter with n-levels was proposed to compensate for reactive power and eliminate the harmonic currents generated by nonlinear loads. The authors introduced a generalized model of the CHB-nL converter that takes into account the effect of the line impedance. Additionally, they proposed an advanced controller that consists of current tracking loop, to ensure that the line current tracks the reference, and outer voltage loops to ensure the regulation and balance of the capacitor voltages involved. A similar article [14] described a control scheme for a STATCOM based on a delta-connected CHB converter. The authors proposed a new feedforward control method to enhance the dynamic performance of the system. The aim of this method was to improve the regulation of zero-sequence circulating current in the delta-connected CHB STATCOM, especially during grid faults or load imbalances, without causing excessive fluctuation in the dc cell capacitor voltage. The proposed method offered significant improvements in the system's dynamic performance. The authors in [15] also proposed a new technique for voltage regulating and balancing. The idea was regulating the three cluster voltages of a star-connected CHB STATCOM to different values, while maintaining balance in the three-phase modulation voltages. This was achieved by decomposing the positive and negative sequence components from the converter voltages to balance the three-phase currents. To ensure the stability of the cluster voltages, the authors extracted the zero-sequence voltage to analyze the active power distribution. The use of an improved model predictive control (MPC) algorithm was suggested in [16] as a means of controlling STATCOM device performance. The authors tried to forecast future STATCOM output current needed to manage designated bus line voltages in accordance with neighboring bus line voltage variations to reduce voltage imbalance. Additionally, they established the MPC state space and goal functions based on neighbors' bus voltages, currents, and transmission line characteristics. Accordingly, the proposed method may be used for wide applications in power systems. In [17], a compensator that combines star and delta segments was proposed to eliminate neutral current, balance loads, and improve power factor. The authors derived a mathematical model based on the load current's phase and sequence components, using symmetrical components theory for load balancing, power factor correction, and neutral current elimination. This study presented the mathematical principle for compensating a star-connected load (with neutral) that is supplied by a balanced three-phase four-wire network, using the theory of symmetrical components. The article [18] suggested a new technique to balance voltages and loads by controlling continuously variable series reactor (CVSR). In more details, by regulating the bias dc circuits of CVSR, the ac reactance was adjusted based on the nonlinear B-H characteristic of the shared ferromagnetic core. Thus, the generated dc bias magnetic flux can then be used to balance the three-phase voltages and reduce the negative impact of any imbalances on the operation and equipment of the distribution system.

The authors in [19] have proposed an algorithm for voltage unbalance detection based on Clark transformation, which converts the three-phase voltages into complex z-plane. The static volt-ampere-reactor compensative (SVC) has the ability to balance the loads and stabilize the electrical power system [20–22]. The authors in [23] used the SVC to balance the load voltages and improve the power factor. The symmetrical component theory was considered to develop the mathematical model for voltage balancing. In [24], a dynamic voltage restorer technique was used together with proportional-integral (PI) controller and phase-locked loop to correct the voltage on the low voltage side. The authors in [25] used the SVC to compensate for the unbalanced three-phase four wires load. A combination of SVC and STATCOM was used to balance the three-phase load voltages in the electrical power system [14, 26]. Several factors must be considered, including accuracy and complexity when control strategies are used for voltage balancing [27, 28]. Also, the time required for algorithm computations must be taken into account. The authors in [29] used the fuzzy logic technique to train artificial neural network (ANN) which controls SVC. The controller needs more than 125 ms to retrieve the voltage balance conditions. The authors in [30] employed the ANN to retrieve the balance conditions at an average time of 60 ms for the voltage unbalance factor (VUF) range of 3.48%–4.68%. Retrieving the voltage balance conditions quickly is a necessity especially for the systems that contain time-varying loads such as electric arc furnaces. In [31], a reactive power compensator was used for this purpose. PSO algorithm is proposed in [32] to find the optimal parameters of the PI controller to retrieve the balance conditions. In [33], genetic algorithm (GA) was used for the same purpose. The GA required more than 130 ms to retrieve the voltage balance. In [34, 35], the PSO was successfully employed in electrical power system applications to retrieve the voltage balance, reduce the voltage sags, and estimate power transformer parameters. In [36], the authors compared between GA and PSO for tuning lead controllers which have three parameters to be optimized. It was concluded that the PSO has a larger mean fitness value along with the generation number compared to GA, especially when the generation continues. In [37], the authors reported some advantages of PSO over other optimization techniques, such as fewer adjustable parameters and more effective memory capability.

In conclusion, the literature review shows that reactive power control using different STATCOMs topologies is an effective strategy to retrieve the voltage balance and the stability of electrical power systems. The majority of the

previously mentioned research works have been focused on controlling the reactive power to retrieve the voltage balance quickly in the three-phase power systems. This will protect the electrical equipment from long-term failures. Additionally, this is vital to enhance the system's dynamic response. Several control techniques have been proposed to solve the problem of voltage balancing and achieve the optimal performance of electrical power systems. Machine learning-based techniques have shown promising results and have the potential to further improve the performance of voltage balancing using STATCOMs. So far, the performance of the proposed solutions is still insufficient and requires further enhancements, such as the system response time and the recovered range of VUF.

In this paper, advanced control strategy using predictive models and optimization algorithm is proposed to control a TCR and retrieve the balance conditions in three-phase power system. PSO is used in offline mode to determine the optimum set of TCR firing angles based on the VUF's smallest fitness value. A mathematical model of a three-phase power system is used for this purpose. The modeled power system comprises a 500 km long transmission line which is divided into three-pi sections to guarantee accurate system response. GPR and SVM models are trained using the optimal firing angles determined by PSO and then used as real-time controllers to recover the voltage balance of the power system. The suggested control strategy has the ability to restore the voltage balance quickly within 20 ms and can cover a wide range of VUF 3.90–8.42%.

The paper is organized as follows: Section 3 describes the three-phase reactive power compensation in electrical power systems. The PSO algorithm and GPR and SVM models are discussed in Section 4. The mathematical model and the prototype of the electrical power system are given in Section 5. Section 6 presents the results and discussion. The contribution of this work is provided in Section 7. Finally, the conclusion of this work is given in Section 8.

3. Three-Phase Reactive Power Compensation

The main reason for using reactive power compensation in electric power networks is to maintain the stability of the power system at different loading conditions [38]. Additionally, it affords many advantages to the power system, such as voltage regulation and load balancing [21, 39]. TCR is commonly used SVC for voltage balancing [40, 41]. It consists of an inductor connected in series with two anti-parallel pair of thyristors. By controlling the thyristor triggering time, the amount of inductive reactance is manipulated to generate the adequate reactive power needed for voltage balancing.

When the three-phase loads become unbalanced (i.e., imbalance of electric power flow in the three-phase load), the compensator has to generate the required reactive power to balance the three-load voltages [42]. If the load is Y-connected, the three load voltages can be calculated by using the following equation:

$$\begin{bmatrix} \overrightarrow{V}_a \\ \overrightarrow{V}_b \\ \overrightarrow{V}_c \end{bmatrix} = \begin{bmatrix} Z_a \overrightarrow{I}_{\mathrm{aL}} \\ Z_b \overrightarrow{I}_{\mathrm{bL}} \\ Z_c \overrightarrow{I}_{\mathrm{cL}} \end{bmatrix} = \mathrm{Z}_y \begin{bmatrix} \overrightarrow{I}_{\mathrm{aL}} \\ \overrightarrow{I}_{\mathrm{bL}} \\ \overrightarrow{I}_{\mathrm{cL}} \end{bmatrix}, \tag{1}$$

where

$$Z_y = \begin{bmatrix} Z_a & 0 & 0 \\ 0 & \mathrm{Z}_b & 0 \\ 0 & 0 & \mathrm{Z}_c \end{bmatrix}, \tag{2}$$

$\overrightarrow{V}_a$, $\overrightarrow{\mathrm{V}}_b$, and $\overrightarrow{V}_c$ represent the load voltages, $\overrightarrow{I}_{\mathrm{aL}}$, $\overrightarrow{I}_{\mathrm{bL}}$, and $\overrightarrow{\mathrm{I}}_{\mathrm{cL}}$ represent the load currents, and Z_a, Z_b, and Z_c represent the Y-connected load impedances.

When the three-phase loads become unbalanced, the three-line currents will also become unbalanced and can be substituted by their symmetrical components as given in the following equation:

$$\begin{bmatrix} \overrightarrow{V}_a \\ \overrightarrow{V}_b \\ \overrightarrow{V}_c \end{bmatrix} = \mathrm{Z}_y \begin{bmatrix} \overrightarrow{I}_{aL1} + \overrightarrow{I}_{aL2} + \overrightarrow{I}_{aL0} \\ \overrightarrow{I}_{bL1} + \overrightarrow{I}_{bL2} + \overrightarrow{I}_{bL0} \\ \overrightarrow{I}_{cL1} + \overrightarrow{I}_{cL2} + \overrightarrow{I}_{cL0} \end{bmatrix}, \tag{3}$$

where $\overrightarrow{I}_{a(L1,L2,L0)}$, $\overrightarrow{I}_{b(L1,L2,L0)}$, and $\overrightarrow{I}_{c(L1,L2,L0)}$ represent positive, negative, and zero sequence components of unbalanced load currents, respectively.

In equation (3), the positive, negative, and zero sequence components are indicated by the subscripts 1, 2, and 0, respectively. The zero-sequence components have no effect on the system balance because they have equal amplitude with zero phase angles from each other. To preserve the balanced three-phase load voltages, the negative-sequence components of the load currents must be eliminated. Therefore, the reactive power compensator should be used to generate the appropriate three susceptances and absorb the negative-sequence components of the load currents leading to balance load voltages. However, to obtain the adequate value of generated compensator susceptance, the TCR firing angles should be calculated accurately. Consequently, an advanced real-time control using GPR and SVM is proposed in this work to perform the previous duties, i.e., calculate the TCR firing angles and retrieve the balance conditions of the electrical power system. Figure 1 shows the proposed controller that utilizes GPR and SVM algorithms to control the reactive power compensator and retrieve balance conditions.

4. The Proposed Integrated Approach

In this work, an advance integrated approach is proposed to control the reactive power and restore the voltage balance in three-phase power systems using the PSO algorithm and SVM-GPR models. The proposed approach can be divided

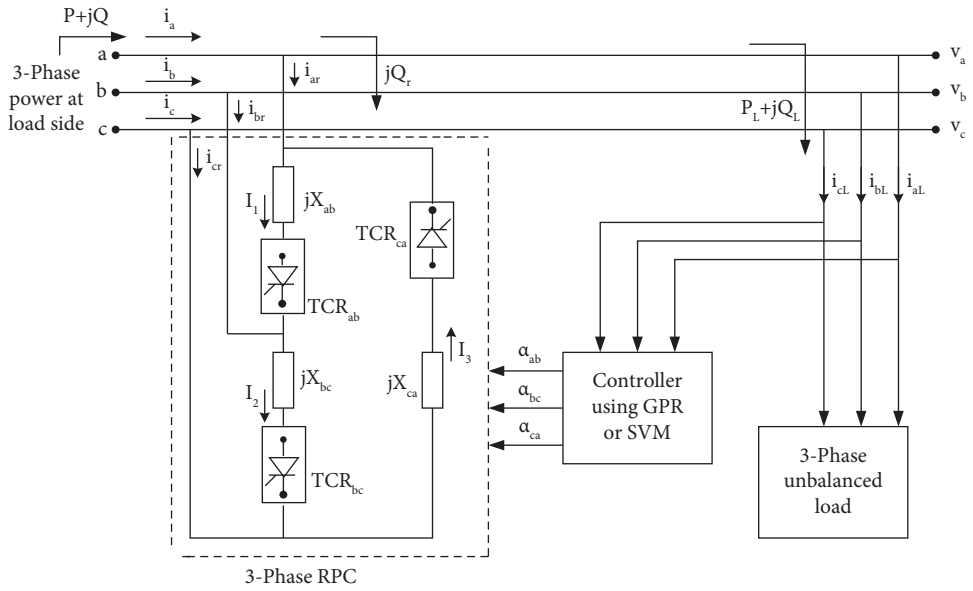

Figure 1: Reactive power compensator.

into three stages. In the first stage, the PSO algorithm is used to determine the optimum set of TCR firing angles, using the steady-state mathematical model of the power system. This stage is executed only in offline mode because using the PSO in online mode will degrade the system's dynamic behavior. This is due to the iterative nature of the PSO computation. Therefore, in the proposed integrated approach, the GPR and SVM are used to control the system in online mode. In the second stage, the optimum firing angles calculated from the PSO in the offline mode are appointed to train the GPR and SVM models. Finally, in the third stage, the GPR and SVM models are used as a real-time controller to restore the voltage balance in online mode.

4.1. Particle Swarm Optimization (PSO) Algorithm. Particle swarm optimization (PSO) was proposed in 1995 by Kennedey and Eberhart. PSO algorithm simulates the swarm behavior in nature. It searches a space of dimension (d) by moving a swarm that consists of n-particles to determine the best solution based on a fitness function. Every particle in the swarm has its own position and velocity [43].

The algorithm starts searching the space of dimension (d) by initializing a swarm with (n) particles, randomly. Then, each particle modifies its position according to its fitness and the fitness of the neighborhood particles as well. The fitness of the particle is evaluated according to the defined cost function to assign the best particle among the current generation which is called the personal best particle (p_{best}). P_{best} is the local particle in the swarm that has the minimum fitness value within the same position in the swarm [44, 45]. The global best particle (g_{best}) of the smallest fitness is found by comparing the fitness values of all personal best particles. In each iteration, the velocity and position of the particles are updated according to equations (4) and (5), respectively [36]. PSO algorithm continues searching in the d-dimensional space until one termination condition is achieved.

$$V_{nd}(\text{iter}) = k\left[wV_{nd}(\text{iter}-1) + c_1 r_1\left(p_{best} - X_{nd}(\text{iter}-1)\right) + c_2 r_2\left(g_{best} - X_{nd}(\text{iter}-1)\right)\right], \tag{4}$$

$$X_{nd}(\text{iter}) = X_{nd}(\text{iter}-1) + V_{nd}(\text{iter}), \tag{5}$$

where

$$k = \frac{2 \times (\text{rand})}{\left|2 - \varphi - \sqrt[2]{\varphi^2 - 4 \times \varphi}\right|},$$
$$\varphi = c_1 r_1 + c_2 r_2, \quad (6)$$
$$w = w_{\max} - \frac{w_{\max} - \mathrm{w}_{\min}}{\mathrm{iter}_{\max}} \times \mathrm{iter},$$

where w represents inertia factor. c_1 and c_2 represent random integers (between 2 and 4). r_1 and r_2 represent random numbers (between 0 and 1). $\mathrm{P}_{\mathrm{best}}$ represents personal best particle. V_{nd} represents the velocity of the n^{th} particle in a space of dimension (d). X_{nd} represents n^{th} particle in a space of dimension (d). g_{best} represents global best particle. rand represents random number (0-1). iter represents sequential number of iterations.

One of the most important aspects when utilizing the PSO algorithm is defining an appropriate fitness function to measure the quality of the solutions. In this paper, the proposed fitness function relies on the VUF of the three-phase load voltages to get the optimal particle that has the smallest fitness value (i.e., smallest VUF).

Figure 2 shows the flowchart of the first stage in the proposed approach. In this stage, the PSO algorithm is used with the mathematical model of a 500 km long electrical power system to find the TCR optimal firing angles required for voltage balancing. The PSO particles represent the TCR firing angles, α_{ab}, α_{bc}, and α_{ca}. The PSO operates when an unbalance load change is detected. The following steps summarise the first stage of the proposed integrated approach.

(1) Strat PSO algorithm by generating a random swarm with n-particles and their velocities. In this paper, the particles and their velocities are given by the following equations, respectively:

$$X_{n3} = [\ \alpha_{\mathrm{ab}} \quad \alpha_{\mathrm{bc}} \quad \alpha_{\mathrm{ca}}\ ], \quad (7)$$

$$V_{n3} = [\ v_1 \quad v_2 \quad v_3\ ], \quad (8)$$

where X_{n3} represents n^{th} particle in a space of 3-dimension (i.e., 3-firing angles of TCR). V_{n3} represents the velocity of the n^{th} 3-dimension particle. α_{ab}, α_{bc}, and α_{ca} represent the firing angles of TCRs. $v_1, v_2,$ and v_3 represent the velocities of the three components of the particle.

(2) Evaluate the three-phase load voltages that correspond to each particle using the mathematical model of the 500 km long electrical power system, and then calculate the fitness (J) of each particle using the following equation:

$$J = \mathrm{VUF} = \frac{V_2}{V_1} \times 100\%, \quad (9)$$

where V_1 represents the positive-sequence voltage and V_2 represents the negative-sequence voltage.

(3) Find $\mathrm{p}_{\mathrm{best}}$ according to the minimum value of fitness (at a minimum value of VUF).

(4) Compare the fitness values of all personal best particles and assign the one with the smallest fitness as the global best particle ($\mathrm{g}_{\mathrm{best}}$).

(5) Update the velocities and particles using equations (4) and (5), respectively.

(6) Repeat steps 2 to 5 until the fitness of VUF for three-phase voltages becomes less than 2%.

(7) Apply the best particle which corresponds to the minimum VUF on the TCR compensator.

4.2. Gaussian Process Regression and Support Vector Machine. The Gaussian processes are probabilistic supervised-machine learning methods that have been extensively utilized in statistical modeling, regression, and pattern classifications [46]. The GPR model performs predictions joining prior knowledge and provides uncertainty measures over predictions [47]. In other words, GPR is a nonparametric kernel-based probabilistic model with a finite collection of random variables with a multivariate distribution. The Gaussian processes have many advantages, such as interpolate observations, adaptive fitting, and kernel versatility. The key points in the GPR can be summarized as follows: Firstly, the next function is updated with new observations. Secondly, finite samples of functions are jointly-Gaussian distributed. Finally, the mean function which is calculated by the posterior distribution of possible functions is used for regression predictions. The regression function modeled by a multivariate Gaussian is given as follows [48]:

$$P\left(\frac{f}{X}\right) = N\left(\frac{F}{\mu, K}\right), \quad (10)$$

where $X = [x_1, \ldots, x_n]$. X is the observed data points. $f = [f(x1), \ldots, f(xn)]$ and $\mu = [m(x1), \ldots, m(xn)]$. m is the mean function, $Kij = k(xi, xj)$. k is a positive definite kernel function.

Support vector machine is a regression and classification tool that uses machine learning theory to increase predictive accuracy and avoid data overfitting problems [48]. SVM uses the hypothesis space of linear functions in a high-dimensional feature space. Additionally, SVM is trained with a learning algorithm from optimization theory that implements a learning bias derived from statistical learning theory [49]. Duality, kernels, convexity, and sparseness are the most major features of SVM, it is one of the best approaches for data modeling and combines generalization control as a technique to control dimensionality. It has been proved that the SVM has the upper hand over the neural network (NN) in regression due to many reasons [50]. SVM gives higher accuracy in comparison with sophisticated neural networks with elaborated features in regression tasks. Additionally, SVM performs better in terms of not

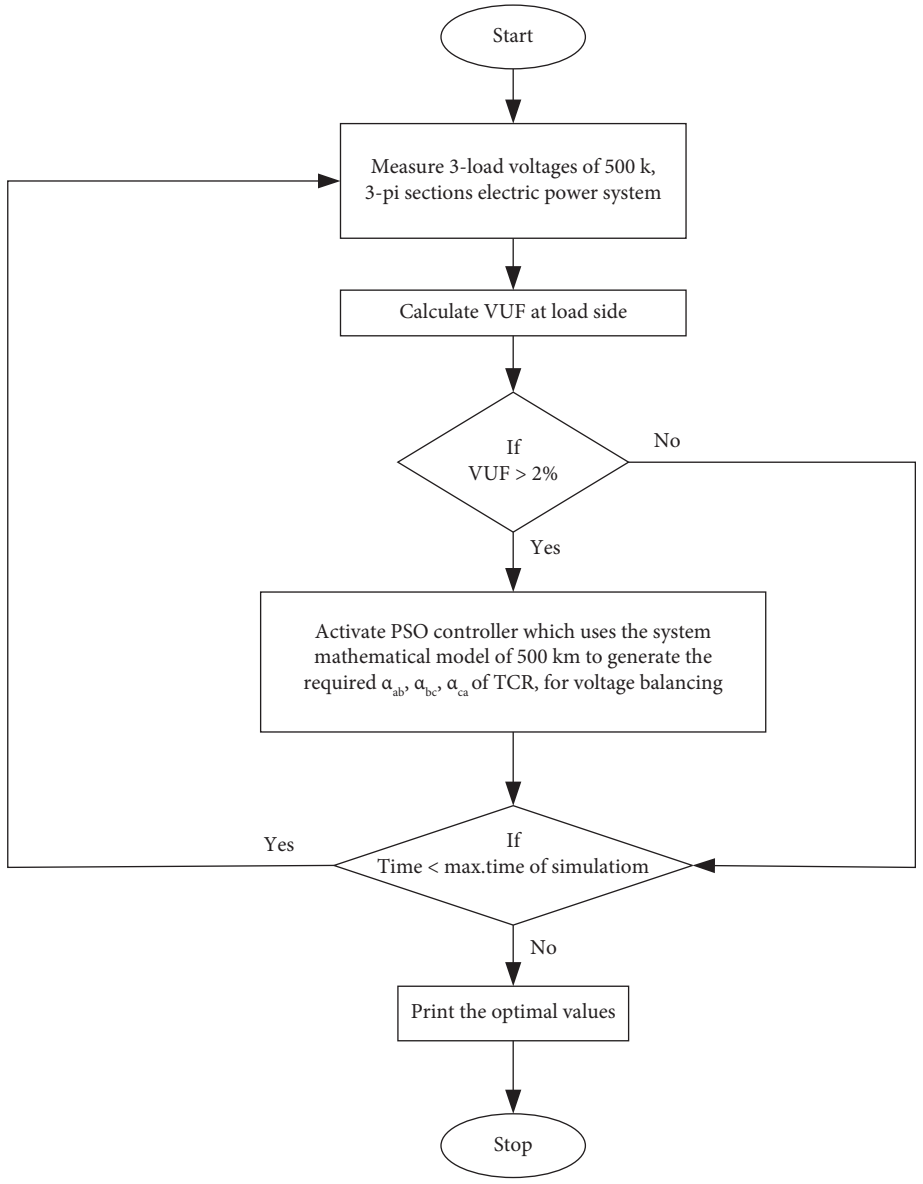

Figure 2: Flowchart of the first stage in the proposed integrated approach.

overgeneralization when the neural networks might end up overgeneralizing easily [49].

5. The Mathematical Model and the Prototype of Electrical Power System

To test the performance of the proposed integrated approach, an electrical power system with a long transmission line is considered and modeled. The general mathematical model was derived in [28] and use in this work for a 500 km long transmission line. This power system consists of a 15 kV 3-phase generator, a step-up transformer at the generator side, step-down transformers at the load side, a 500 km long transmission line divided into three-pi sections, and delta connected load. Table 1 shows the components specifications in the modeled power system. The mathematical model of the power system is generated, built, and simulated using MATLAB SIMULINK. Figure 3 shows the block diagram of the modeled power system with the PSO algorithm. Moreover, an experimental setup of the power system prototype is built to support the simulated results and validate the ability of the proposed integrated approach in retrieving the voltage balance conditions successfully. The prototype consists of the following equipment: three-phase voltage source of 178 V, the equivalent transmission line divided into 3 π-section networks, three-phase inductive load, and data acquisition (DAQ) device. The experimental setup is shown in Figure 4.

6. Results and Discussions

As mentioned in Section 3, the proposed approach is divided into three stages. In stage one, the PSO algorithm is used to determine the optimum set of TCR firing angles in offline

Table 1: The components' specifications in the modeled power system.

Power plant	Step-up transformer	Transmission line	Step-down transformer
Capacity: 650 MW Generator: (i) 160 MVA (ii) 15 kV	Ratio: 1 : 28.5	(i) Long: 500 km (ii) Three-pi sections (iii) Each section: (500/3) km $R = 8.5\ \Omega$/section $X_L = 40\ \Omega$/section $X_C = 23.466\ \Omega$/section	4-stages At ratios: 1 : 0.33 1 : 0.25 1 : 0.333 1 : 0.0345

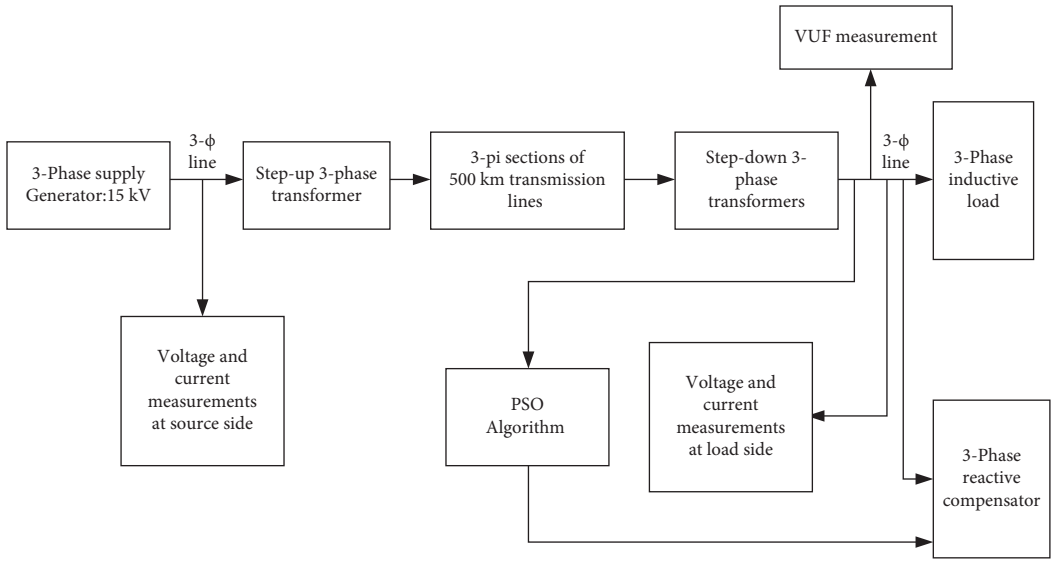

Figure 3: Block diagram of the modeled power system with the PSO algorithm.

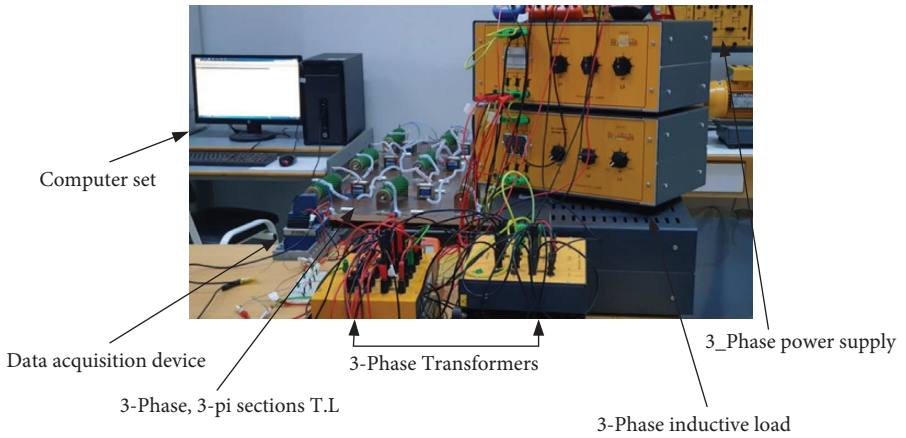

Figure 4: The experimental setup for the power system prototype.

mode. These firing angles are used in stage two to train the GPR and SVM models. In the third stage, the GPR and SVM models are used as real-time controllers to retrieve the voltage balance. Accordingly, in this section, the results and discussions will be introduced for each stage individually.

6.1. The Results and Discussion in Stage One. Many unbalance cases were created to evaluate the ability of the proposed PSO algorithm for restoring the voltage balance in the load side of the system. Table 2 shows the results for different loading conditions covering a wide range of VUF. Table 2 includes the VUF values before and after PSO action, the optimal firing angles generated by the PSO algorithm, and the time needed to retrieve the balance conditions measured from the PSO initiating time. As indicated in Table 2, the average value of VUF after activating the PSO is 0.717% which is lower and better than the recommended value (i.e., 3%). Thus, the results prove the capability of the proposed PSO algorithm in recovering the system balance conditions

Table 2: The results from the simulation model for different unbalance cases.

Before the action of PSO	After the action of PSO				
	TCR firing angles (degrees)				
VUF (%)	α_{ab}	α_{bc}	α_{ca}	VUF (%)	Time needed by the PSO to retrieve balance conditions (ms)
3.576%	162.6°	156.5°	102.1°	0.815%	22
2.537%	179.3°	125.9°	110.5°	0.347%	21.09
3.055%	132.5°	152.9°	106.6°	0.593%	22.18
3.219%	121.8°	127.6°	94.6°	0.326%	22.41
4.047%	128.3°	153.3°	98.16°	0.164%	22.16
3.776%	128.9°	139.8°	97.72°	0.038%	22.10
4.144%	169.1°	174.1°	103.0°	0.062%	22.20
4.332%	169.9°	148.2°	100.6°	0.168%	22.14
5.456%	179.9°	118.5°	90.0°	0.292%	22.19
4.754%	153.1°	122.5°	93.3°	0.265%	22.15
6.348%	179.7°	114.5°	91.0°	1.319%	22.18
5.782%	179.4°	116.8°	92.0°	0.671%	22.16
6.776%	179.4°	113.1°	90.0°	1.812%	25.30
6.906%	179.70°	112.80°	90.0°	1.944%	35.90
6.971%	179.1°	109.3°	90.0°	1.946%	31.40
The average value of VUF after the action PSO				0.717%	—
The average value of time needed by the PSO to retrieve balance conditions					23.837

and achieving very low VUF values. In addition, it can be noted from Table 2 that the time needed by the PSO to retrieve the system balance conditions in some cases exceeded 30 ms. This long delay in the PSO response will degrade the system's dynamic behavior. Consequently, the PSO is used in the offline mode only.

6.2. The Results and Discussion in Stage Two. The optimum set of TCR firing angles generated by the PSO in stage one was used to train GPR and SVM models. The input data for these models are the three load unbalance voltages and the VUF, while the output data of these models are the three firing angles of the TCR compensator needed for voltage balancing. The performance of the trained GPR and SVM models is shown in Figures 5 and 6, respectively. The regression factor (R^2), which indicates the model's ability to produce the desired output, is 0.95 and 0.93 for GPR and SVM models, respectively. The root mean square error (RMSE), which shows the model's ability to track the data points, is 0.084772 and 0.099518 for GPR and SVM, respectively. The results show that the GPR and SVM models have the ability to track the data points and produce the desired output efficiently. However, at this stage, the GPR model introduced a slightly better performance than the SVM.

6.3. The Results and Discussion in Stage Three. Several tests were conducted to demonstrate, assess, and validate the feasibility and effectiveness of the proposed integrated approach in restoring the system voltage balance. During these tests, the three loads were changed deliberately and asymmetrically to create a wide range of unbalanced voltages. The tests were conducted using both the simulation and practical models.

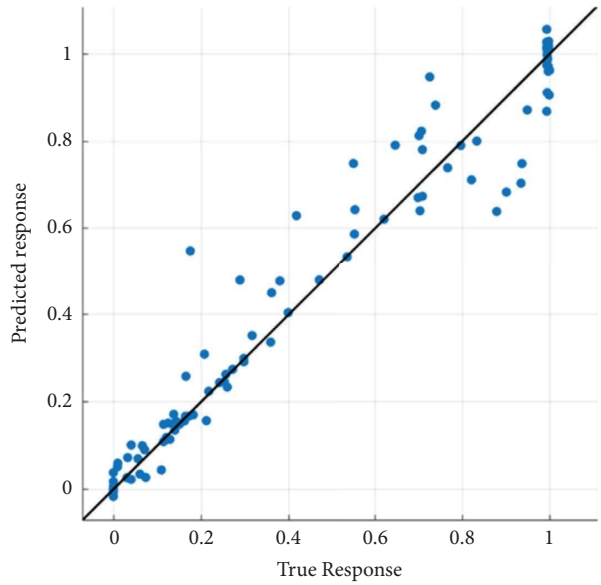

Figure 5: The regression graph of the GPR model.

Three tests were conducted using the simulation and practical models. The first and second tests were conducted using the simulation model, while the third test was conducted using the practical model. In the first test, many unbalance cases were created to test the ability of the GPR and SVM models in recovering the voltage balance for different loading conditions covering a wide range of VUF. Tables 3 and 4 show the results of this test when using GPR and SVM models, respectively. These tables include the TCR firing angles generated by GPR and SVM models, the VUF values, and the three load voltages before and after the model's action. It can be noted from these tables that the

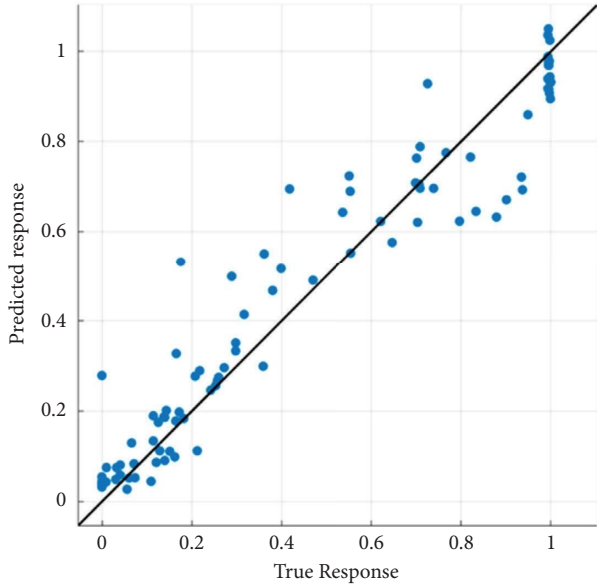

Figure 6: The regression graph of the SVM model.

Table 3: GPR results.

Before GPG action				After GPR action						
Load voltages			VUF%	TCR firing angles			Load voltages			VUF%
Va	Vb	Vc		α^{o}_{ab}	α^{o}_{bc}	α^{o}_{ca}	Va	Vb	Vc	
0.976	0.974	1.05	5.57	155.98	164.56	103.46	1.004	1.002	0.994	0.539
0.987	0.971	1.04	4.73	154.31	156.65	105.06	0.999	0.999	1.002	0.191
0.959	0.987	1.053	5.608	178.75	120.34	91.75	0.994	1	1.005	0.589
1.03	0.998	0.971	3.90	108.55	141.73	168.87	0.995	1.008	0.996	0.791
1.061	0.949	0.989	6.985	90.16	179.21	109.71	1.005	1.003	0.991	0.842
0.959	1.054	0.989	5.76	170.21	95.68	148.09	0.997	0.999	1.003	0.357
1.035	1.034	0.93	7.19	94.28	92.57	159.49	1.006	0.996	0.997	0.614
0.956	1.032	1.011	4.49	151.08	94.33	117.24	1.002	0.999	0.1.001	0.308
0.969	0.98	1.05	5.71	157.50	128.25	93.582	0.995	1.005	1.001	0.575
0.945	0.984	1.06	7.48	179.74	114.01	90.44	0.99	0.996	1.01	1.09
0.979	0.969	1.05	5.93	170.36	161.15	99.45	0.998	1.001	1.001	0.135
0.986	0.976	1.03	3.83	149.78	149.64	105.65	0.995	1.003	1.001	0.415
0.944	0.985	1.071	8.22	179.51	111.70	89.96	0.997	0.994	1.018	0.981
0.974	1.057	0.968	6.21	132.73	91.371	179.96	0.999	1.004	0.996	0.511
0.991	1.069	0.939	8.42	112.69	90.91	178.67	0.999	1.011	0.989	0.771
Average of VUF			6.002			Average of VUF				0.580

average value of VUF before the model's actions is 6.002%. As indicated in Table 3, the average value of the VUF is reduced to 0.580% by using the GPR model. While, as indicated in Table 4, the SVM reduced it to 2.041% which is lower and better than the recommended value (i.e., 3%). Thus, the results in Tables 3 and 4 prove the capability of the GPR and SVM models in recovering the system balance conditions efficiently and achieving very low VUF values. Additionally, the results revealed that the GPR outperforms the SVM by achieving low VUF values.

In the second test, an unbalance case was created to assess the system time response and demonstrate the three-phase load voltages. The test case scenario is as follows: starting the electrical power system with balanced conditions during the time interval from 0 to 0.1 sec, then making unbalance change in the three-phase loads exactly at 0.1 sec, and finally initiating the GPR or SVM controller at 0.15 sec. Figures 7 and 8 illustrate the effect of GPR and SVM controllers, respectively, on the three load voltages when the VUF is 6.985%. It is noted that the GPR and SVM controller recovered the balance conditions of the power system accurately within a very narrow time interval. Additionally, The VUF is reduced from 6.985% to 0.842% and from 6.985% to 1.752% using GPR and SVM, correspondingly.

In the third test, which was conducted using the practical model, another unbalance case was created to validate the simulation results in the second test. The unbalance change in the three-phase loads is initiated at 0.05 sec, and GPR or SVM controller is activated at 0.1 sec. Figures 9 and 10 illustrate the effect of GPR and SVM controllers, respectively,

Table 4: SVM results.

Before SVM action				After SVM action						
Load voltages			VUF%	TCR firing angles			Load voltages			VUF%
Va	Vb	Vc		α^{o}_{ab}	α^{o}_{bc}	α^{o}_{ca}	Va	Vb	Vc	
0.976	0.974	1.05	5.57	147.57	136.61	116.38	0.993	0.983	1.018	2.005
0.987	0.971	1.04	4.73	150.05	135.80	114.39	0.998	0.983	1.018	2.058
0.959	0.987	1.053	5.608	165.33	115.57	101.97	0.993	0.983	1.021	2.187
1.03	0.998	0.971	3.90	111.74	129.84	151.53	1.007	0.984	0.994	2.105
1.061	0.949	0.989	6.985	100.13	178.10	116.46	1.017	0.992	0.99	1.752
0.959	1.054	0.989	5.76	142.37	97.35	136.07	0.992	1.007	0.995	1.881
1.035	1.034	0.93	7.19	105.26	168.15	130.42	1.004	1.019	0.977	2.464
0.956	1.032	1.011	4.49	150.32	99.63	122.96	0.996	0.998	1.005	0.473
0.969	0.98	1.05	5.71	159.28	121.87	107.64	0.992	0.986	1.021	2.178
0.945	0.984	1.06	7.48	171.39	112.40	96.13	0.988	0.989	1.022	2.216
0.979	0.969	1.05	5.93	154.12	132.03	110.43	0.999	0.98	1.02	2.314
0.986	0.976	1.03	3.83	148.80	135.27	116.23	0.996	0.987	1.018	1.904
0.944	0.985	1.071	8.22	175.02	111.36	92.74	0.986	0.99	1.023	2.296
0.974	1.057	0.968	6.21	133.49	96.03	154.37	0.995	1.014	0.984	1.894
0.991	1.069	0.939	8.42	119.25	103.50	173.49	0.994	1.032	0.987	2.895
Average of VUF			6.002			Average of VUF				2.041

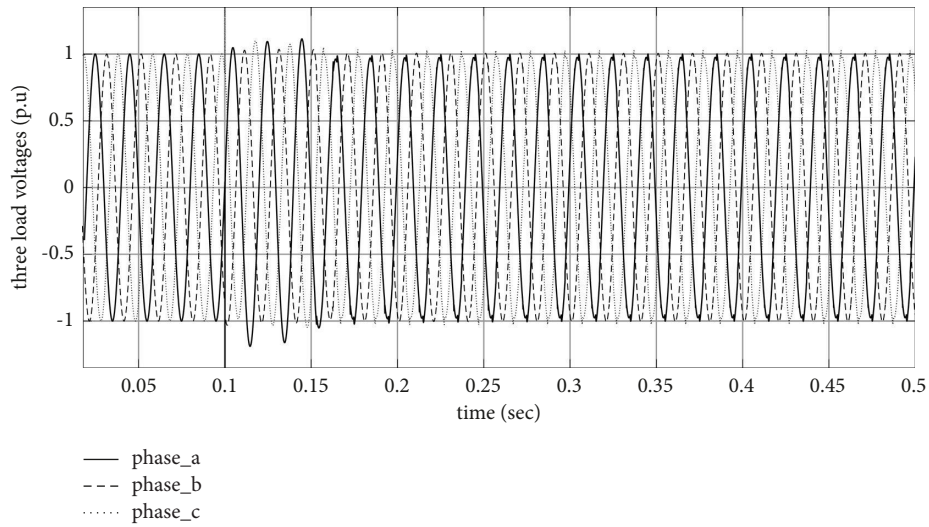

Figure 7: Waveforms of three-phase load voltages for the unbalanced case of 6.985% VUF which is reduced to 0.842% after using the proposed GPR controller.

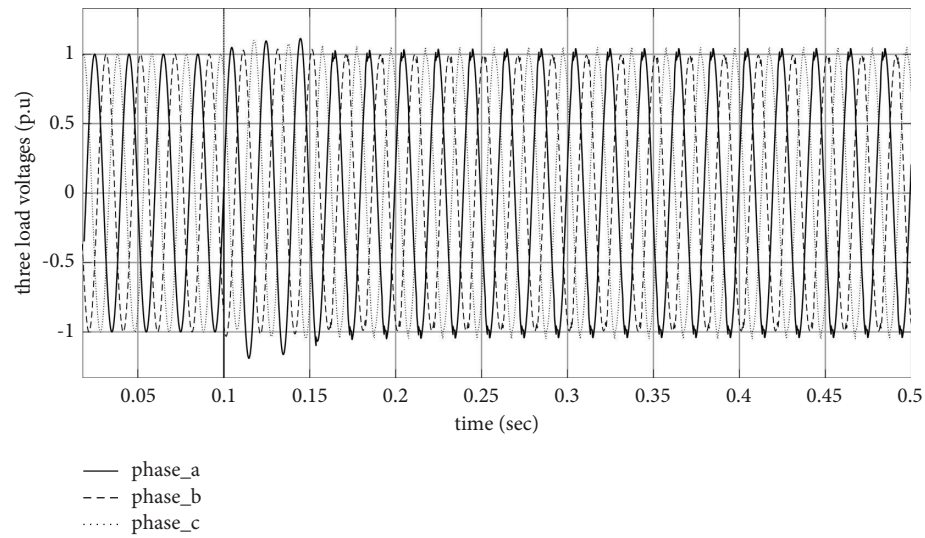

Figure 8: Waveforms of three-phase load voltages for the unbalanced case of 6.985% VUF which is reduced to 1.752% after using the proposed SVM controller.

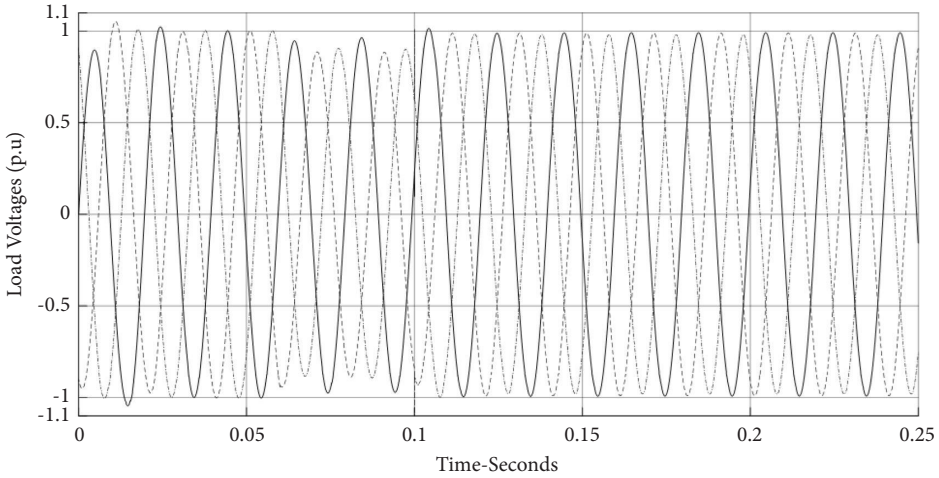

Figure 9: Three-phase load voltages when using GPR controller to reduce the VUF value from 5.69% to 1.64%.

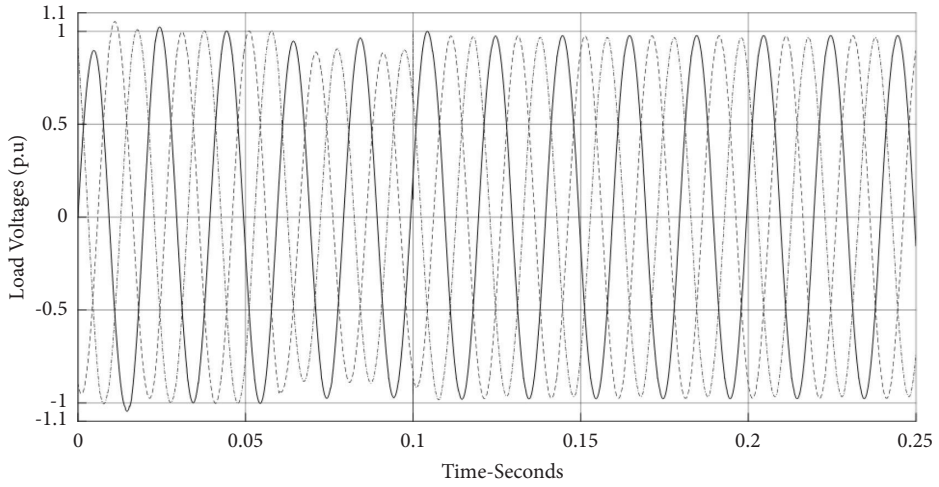

Figure 10: Three-phase load voltages when using SVM controller to reduce the VUF value from 5.69% to 2.03%.

on the three load voltages when the VUF is 5.69%. It can be observed from these figures that the GPR and SVM controllers recovered the balance conditions of the power system accurately within a very narrow time interval. Additionally, The VUF is reduced from 5.69% to 1.64% and from 5.69% to 2.03% using GPR and SVM, correspondingly. In conclusion, the results from the three tests proved the ability of the proposed integrated approach to balance the three-load voltages quickly and achieving very low VUF values.

7. Contribution to Knowledge

Table 5 introduces a brief comparison between the state-of-the-art techniques for voltage balancing in three-phase power systems mentioned in Section 3 and the proposed integrated approach. Accordingly, the contributions of knowledge in this paper are as follows:

(1) In the proposed integrated approach, GPR and SVM models are trained using the optimum data set of firing angles generated from the PSO algorithm. These firing angles are required to drive the TCR compensator and restore the voltage balance in the three-phase power system. These optimum values enhanced the performance of the trained GPR and SVM models and achieved high R^2 factor and low RMSE.

(2) The proposed integrated approach retrieved the balanced conditions in the electrical power systems successfully by achieving a fast response time of only 20 ms. Indeed, this is the shortest response time among the methods proposed in the literature. Therefore, the proposed approach enhanced the system's dynamic behavior.

(3) The proposed integrated approach can solve the voltage unbalance problem and cover a wide range of VUF between 3.90% and 8.42%. This VUF range is wider than the ranges achieved in the literature.

(4) The proposed integrated approach obtained the best performance for a three-phase power system and

Table 5: A comparison between the proposed PSO technique and other techniques.

Comparison criteria	Work in [18] published in 2023	Work in [13] published in 2023	Work in [28] published in 2020	Work in [33] published in 2020	Work in [30] published in 2019	The proposed approach	Notes
Power compensator	CVSR	3ph-CHB multilevel converter	TCR	TSC-TCR	TCR	TCR	The majority of these researches utilized TCR to solve the problem of unbalanced voltages
Algorithm	Regulating the bias dc circuits of CVSR. The ac reactance was adjusted based on the B-H of the core. The generated dc bias magnetic flux is used to balance the three-phase voltages	Decoupling coordinates transformation to design three loops, a current tracking loop, a voltage regulation loop, and a voltage balance loop	PSO	Triangular membership function	The firing angles of the TCR required to retrieve the system balance conditions were determined by trial and error	PSO	The proposed PSO algorithm uses the mathematical model of the power system to determine the required set of TCR firing angles. Thus, it is more accurate compared to the ones in [28, 30]. Additionally, this operation is performed offline which make the proposed approach faster than the one proposed in [13, 18]
Controller	Iterative process depending on measuring the load voltages, searching for the dc biases, and calculating the relative error between the voltages	Model based PI and PR closed loop controller	ANN	Fuzzy logic	ANN	GPR and SVM	SVM and GPR have the upper hand over the ANN in regression. They give higher accuracy and consume less time comparable to sophisticated ANN with elaborated features in regression tasks
VUF range	<5%	Undefined	3.44–6.93%	Undefined	3.48–4.68%	3.90–8.42%	The proposed approach covers a wider range of VUF
Average response time (at 50 Hz)	>60 ms	>200 ms	57.92 ms	>43 ms	60 ms	20 ms	The response time of the proposed approach is the shortest time with just 20 ms

restored the voltage balance at an average VUF of 0.580%

8. Conclusion

In this paper, an advance integrated approach is proposed to control the reactive power and restore the voltage balance in three-phase power systems using the PSO algorithm and SVM-GPR models. The PSO algorithm is used to determine the optimum set of TCR firing angles required for voltage balancing in offline mode, these firing angles are then used to train the GPR and SVM regression models; finally, the models are used as a real-time controller to restore the voltage balance in the online mode. Simulation and physical models for the electrical power system were built. In addition, three tests with different unbalance cases were conducted to validate the proposed integrated approach. The results have revealed the superiority of the proposed advanced approach over others mentioned in the literature and the ability of this approach to retrieve the voltage balance conditions quickly (within 20 ms) with a wide range of VUF (3.90–8.42%).

Data Availability

The data used in this study are available from the corresponding author upon request.

Conflicts of Interest

The authors declare that they have no conflicts of interest.

Acknowledgments

This research work was funded by Philadelphia University, Amman-Jordan.

References

[1] F. Nejabatkhah, Y. Li, and B. Wu "Control, "Strategies of three-phase distributed generation inverters for grid unbalanced voltage compensation," *IEEE Transactions on Power Electronics*, vol. 31, no. 7, pp. 5228–5241, 2016.

[2] I. Al-Naimi, J. Ghaeb, M. Baniyounis, and M. Al-Khawaldeh, "Fast detection technique for voltage unbalance in three-phase power system," *International Journal of Power Electronics and Drive Systems*, vol. 12, no. 4, p. 2230, 2021.

[3] T. Nguyen, D. Vo, H. Van Tran, and L. Van Dai, "Optimal dispatch of reactive power using modified stochastic fractal search algorithm," *Complexity*, vol. 2019, Article ID 4670820, 28 pages, 2019.

[4] J. Wadhawan, U. Pandey, M. Yadav, and A. Kesarwani, "A Review on Power Quality Problems and Improvement Techniques," *International Journal of Engineering Research and Technology (IJERT)*, vol. 8, no. 10, 2020.

[5] M. Tucci, L. Meng, J. M. Guerrero, and G. Ferrari-Trecate, "Stable current sharing and voltage balancing in DC microgrids: a consensus-based secondary control layer," *Automatica*, vol. 95, pp. 1–13, 2018.

[6] C. Ciontea and F. Iov, "A study of load imbalance influence on power quality assessment for distribution networks," *Electricity*, vol. 2, no. 1, pp. 77–90, 2021.

[7] J. Ghaeb, D. Ragab, and I. Al-Naimi, "Fast correction of voltage unbalance factor in three-phase power system using neural network," in *Proceedings of the 11th International Symposium on Mechatronics and its Applications (ISMA)*, Sharjah, UAE, March 2018.

[8] A. Nour, A. Helal, M. El-Saadawi, and A. Hatata, "A control scheme for voltage unbalance mitigation in distribution network with rooftop PV systems based on distributed batteries," *International Journal of Electrical Power & Energy Systems*, vol. 124, Article ID 106375, 2021.

[9] M. Ayala-Chauvin, B. Kavrakov, J. Buele, and J. Varela-Aldás, "Static reactive power compensator design, based on three-phase voltage converter," *Energies*, vol. 14, no. 8, p. 2198, 2021.

[10] R. Sadiq, Z. Wang, C. Chung, C. Zhou, and C. Wang, "A review of STATCOM control for stability enhancement of power systems with wind/PV penetration: existing research and future scope," *International transactions on Electrical Energy Systems*, vol. 31, no. 11, 2021.

[11] A. Obais and A. Mukheef, "Load current balancing for 4-wire systems using harmonic treated TCR based SVCs," *International Journal of Power Electronics and Drive Systems*, vol. 13, no. 3, pp. 1922–1950, 2022.

[12] M. Wara and A. Rahim, "Supercapacitor E-STATCOM for power system performance enhancement," in *Proceedings of the 2019 International Conference on Robotics, Electrical and Signal Processing Techniques (ICREST)*, pp. 69–73, Dhaka, Bangladesh, January 2019.

[13] A. Valdez-Fernandez, G. Escobar, D. Campos-Delgado, and M. Hernandez-Ruiz, "Model-based control strategy for the three-phase n-level CHB multilevel converter" International," *Journal of Electrical Power & Energy Systems*, vol. 147, 2023.

[14] J. Jung, J. Lee, S. Sul, G. T. Son, and Y. Chung, "DC capacitor voltage balancing control for delta-connected cascaded H-bridge STATCOM considering unbalanced grid and load conditions," *IEEE Transactions on Power Electronics*, vol. 33, no. 6, pp. 4726–4735, 2018.

[15] D. Lu, S. Wang, J. Yao, T. Yang, and H. Hu, "Cluster voltage regulation strategy to eliminate negative-sequence currents under unbalanced grid for star-connected cascaded H-bridge STATCOM," *IEEE Transactions on Power Electronics*, vol. 34, no. 3, pp. 2193–2205, 2019.

[16] A. Emam, A. Azmy, and E. Rashad, "Enhanced model predictive control-based STATCOM implementation for mitigation of unbalance in line voltages," *IEEE Access*, vol. 8, pp. 225995–226007, 2020.

[17] A. Ojo, K. Awodele, and A. Sebitosi, "Load compensation in a three-phase four wire distribution system considering unbalance, neutral current elimination and power factor improvement," in *Proceedings of the 2019 Southern African Universities Power Engineering Conference/Robotics and Mechatronics/Pattern Recognition Association of South Africa (SAUPEC/RobMech/PRASA)*, pp. 389–394, Bloemfontein, South Africa, January 2019.

[18] M. Hayerikhiyavi and A. Dimitrovski, "Voltage balancing using continuously variable series reactor," in *Proceedings of the 2023 IEEE Texas Power and Energy Conference (TPEC)*, pp. 1–5, College Station, TX, USA, February 2023.

[19] M. Sun, S. Demirtas, and Z. Sahinoglu, "Joint voltage and phase unbalance detector for three phase power systems," *IEEE Signal Processing Letters*, vol. 20, no. 1, pp. 11–14, 2013.

[20] J. Ghaeb and O. Aloquili, "High performance reactive control for unbalanced three-phase load," *European Transactions on Electrical Power*, vol. 20, no. 6, pp. 710–722, 2010.

[21] F. Igbinovia, G. Fandi, J. Svec, and Z. Muller, "J. Tlusty "Comparative review of reactive power compensation technologies"" in *Proceedings of the IEEE 16th International Scientific Conference on Electric Power Engineering (EPE)*, Koutynad Desnou, Czech Republic, May 2015.

[22] J. Ghaeb, M. AlKayyali, and T. Tutunji, "Wide range reactive power compensation for voltage unbalance mitigation in electrical power systems," *Electric Power Components and Systems*, vol. 49, no. 6-7, pp. 715–728, 2021.

[23] S. Das, D. Chatterjee, and S. Goswami, "A GSA-based modified SVC switching scheme for load balancing and source power factor improvement," *IEEE Transactions on Power Delivery*, vol. 31, no. 5, pp. 2072–2082, 2016.

[24] O. Taiwo, R. Tiako, and I. Davidson, "An improvement of voltage unbalance in a low voltage 11/0.4 kV electric power distribution network under 3-phase unbalance load condition using dynamic voltage restorer," in *Proceedings of the IEEE Power Engineering Society Conference and Exposition in Africa*, pp. 126–131, Accra, Ghana, June 2017.

[25] F. Quintela, J. Arevalo, R. Redondo, and N. Melchor, "Four-wire three-phase load balancing with Static VAR Compensators," *International Journal of Electrical Power & Energy Systems*, vol. 33, no. 3, pp. 562–568, 2011.

[26] Y. Shi, B. Liu, Y. Shi, and S. Duan, "Individual phase current control based on optimal zero-sequence current separation for a star-connected cascade STATCOM under unbalanced conditions," *IEEE Transactions on Power Electronics*, vol. 31, no. 3, pp. 2099–2110, 2016.

[27] J. Jayachandran and R. Murali Sachithanandam, "ANN based controller for three phase four leg shunt active filter for power quality improvement," *Ain Shams Engineering Journal*, vol. 7, no. 1, pp. 275–292, 2016.

[28] M. Alkayyali and J. Ghaeb, "Hybrid PSO–ANN algorithm to control TCR for voltage balancing," *IET Generation Transmission & Distribution*, vol. 14, no. 5, pp. 863–872, 2020.

[29] D. Kulkarni and G. Udupi, "ANN-based SVC switching at distribution level for minimal-injected harmonics," *IEEE Transactions on Power Delivery*, vol. 25, no. 3, pp. 1978–1985, 2010.

[30] D. Ragab, J. Ghaeb, and I. Al Naimi, "Enhancing the response of thyristor-controlled reactor using neural network," *International Transactions on Electrical Energy Systems*, vol. 29, no. 12, pp. 1–16, 2019.

[31] A. Kavousi-Fard, A. Khosravi, and S. Nahavandi, "Reactive power compensation in electric arc furnaces using prediction intervals," *IEEE Transactions on Industrial Electronics*, vol. 64, no. 7, pp. 5295–5304, 2017.

[32] S. Eilaghi, A. Ahmadian, and M. Golkar, "Optimal voltage unbalance compensation in a micro-grid using PSO algorithm," in *Proceedings of the IEEE 7th Power India International Conference (PIICON)*, pp. 25–27, Bikaner, India, November 2016.

[33] K. Shah, S. Arya, and D. Harwani, "Reactive power compensation by TSC-TCR using fuzzy logic controller," in *Proceedings of the International Conference on Data Science, Machine Learning and Applications*, pp. 1226–1236, Springer Proceedings, Hyderabad, India, May 2020.

[34] H. Illias, K. Mou, and A. Bakar, "Estimation of transformer parameters from nameplate data by imperialist competitive and gravitational search algorithms," *Swarm and Evolutionary Computation*, vol. 36, pp. 18–26, 2017.

[35] D. Kumar, S. Sasitharan, M. Mishra, and B. Kumar, "Unbalanced voltage sag correction with dynamic voltage restorer using particle swarm optimization," in *Proceedings of the 2008 Annual IEEE India Conference*, pp. 400–405, Kanpur, India, December 2008.

[36] Z. Abo-Hammour, M. Al Saaideh, M. Alkayyali, and H. Khasawneh, "Optimal design of lead compensator using nature-inspired algorithms," in *Proceedings of the IEEE Jordan International Joint Conference on Electrical Engineering and Information Technology (JEEIT)*, pp. 40–45, Amman, Jordan, April 2019.

[37] Y. del Valle, G. Venayagamoorthy, S. Mohagheghi, J. Hernandez, and R. Harley, "Particle swarm optimization: basic concepts, variants and applications in power systems," *IEEE Transactions on Evolutionary Computation*, vol. 12, no. 2, pp. 171–195, 2008.

[38] Y. Chang, "Multi-objective optimal SVC installation for power system loading margin improvement," *IEEE Transactions on Power Systems*, vol. 27, no. 2, pp. 984–992, 2012.

[39] F. Alhasawi and J. V. Milanovic, "Techno-economic contribution of FACTS devices to the operation of power systems with high level of wind power integration," *IEEE Transactions on Power Systems*, vol. 27, no. 3, pp. 1414–1421, 2012.

[40] R. Gutman, J. Keane, M. Rahman, and O. Veraas, "Application and operation of a static var system on a power system-americal electric power experience Part II: equipment design and installation," *IEEE Transactions on Power Apparatus and Systems*, vol. 104, no. 7, pp. 1875–1881, 1985.

[41] F. Aboytes, G. Arroyo, and G. Villa, "Application of static var compensators in longitudinal power systems," *IEEE Transactions on Power Apparatus and Systems*, vol. 102, no. 10, pp. 3460–3466, 1983.

[42] J. Chen, W. Lee, and M. Chen, "Using a static VAR compensator to balance a distribution system," *IEEE Transactions on Industry Applications*, vol. 35, no. 2, pp. 298–304, 1999.

[43] X. Yang, "Particle swarm optimization," in *Nature-inspired Optimization Algorithms*, pp. 99–110, Elsevier, Amsterdam, The Netherlands, 2014.

[44] N. Singh and S. Singh, "Personal best position particle swarm optimization," *Journal of Applied Computer Science Methods*, vol. 12, no. 6, 2012.

[45] S. Huang, N. Tian, Y. Wang, and Z. Ji, "Particle swarm optimization using multi-information characteristics of all personal-best information," *Springer Plus*, vol. 5, 1632 pages, 2016.

[46] J. Wang, "An intuitive tutorial to Gaussian processes regression," Report from Queen's University, Queen's University, Kingston, Canada, 2021.

[47] N. Zhang, J. Zhong, and K. Leatham, "Gaussian process regression method for classification for high-dimensional data with limited samples," in *Proceedings of the 8th International Conference on Information Science and Technology*, Granada-Spain, June 2018.

[48] R. Monteiro, M. Cerrada, D. Cabrera, R. Sánchez, and C. Bastos-Filho, "Using a support vector machine based decision stage to improve the fault diagnosis on gearboxes," *Computational Intelligence and Neuroscience*, vol. 2019, Article ID 1383752, 13 pages, 2019.

[49] D. Basak and S. Pal, *Support Vector Regression" statistics and Computing Journal*, vol. 11, no. 10, 2007.

[50] W. Niu, Z. Feng, B. Feng, Y. Min, C. Cheng, and J. Z. Zhou, "Comparison of multiple linear regression, artificial neural network, extreme learning machine, and support vector machine in deriving operation rule of hydropower reservoir," *Water*, vol. 11, no. 1, p. 88, 2019.